

# Chiral networks in twisted graphene bilayers under interlayer bias

Pablo San-Jose<sup>1</sup>, Elsa Prada<sup>2</sup>

<sup>1</sup>*Instituto de Ciencia de Materiales de Madrid (ICMM-CSIC), Cantoblanco, 28049 Madrid, Spain*

<sup>2</sup>*Departamento de Física de la Materia Condensada,  
Universidad Autónoma de Madrid, Cantoblanco, 28049 Madrid, Spain*

(Dated: March 4, 2022)

A twisted graphene bilayer exhibits a triangular Moiré pattern in the local stacking, that smoothly alternates between the three basic types AA', AB' and BA'. Under an interlayer bias  $U$ , the latter two types develop a spectral gap, characterised by opposite valley Chern numbers. We show that for large enough Moiré periods and bias (angles smaller than  $\sim 0.2^\circ$  at  $U \sim 90$  meV) these regions become depleted electronically, and topologically protected chiral modes appear at their boundaries. This gives rise to a delocalised chiral network of the Chalker-Coddington type, composed of valley current vortices. Simultaneously, a discrete set of localised states at resonant energies develop. Clear signatures of this exotic electronic state are predicted to arise in the spectrum and the optical conductivity.

In spite of graphene being a zero gap semiconductor[1], the practical difficulty to induce a finite gap has hindered its potential for nanoelectronics applications. In this regard, graphene bilayers were shown early on to possess one significant practical advantage over their monolayer counterpart. For Bernal-type stacking of the two layers (also known as AB' or BA' stacking [2]), a band gap can be opened around each valley by applying an electric bias between the two layers [3, 4]. Gaps up to 250 meV have been achieved experimentally [5, 6]. This property allows a graphene bilayer to be electrically tuned into a very high mobility semiconductor [7], greatly extending its potential for applications.

The gap tunability of graphene bilayers is intriguing also from a fundamental point of view. Firstly, it depends critically on the precise AB' or BA' interlayer stacking. An AA' bilayer, for example, is a good metal for any reasonable interlayer bias. Secondly, the gap can be made to “change sign” by inverting the bias  $U$  into  $-U$ . Performing such an inversion between two adjacent regions in space gives rise to two topologically protected chiral (TPC) modes per valley, that flow without resistance along the interface between the two regions [8] [9]. Analogous TPC channels arise in a range of systems, in which the gapped local band structure changes topology across a boundary, e.g. at the edges of Hall bars, or the surface of topological insulators [10, 11]. Lastly, and rather surprisingly, a change of the topology of a tuned gap can be induced also with a *uniform* bias  $U$  by smoothly transitioning from AB' to BA' stackings [12], which are related by mirror symmetry. This can be achieved by applying a different strain to each layer, and also gives rise to TPC modes.

In this work we address the problem of the formation of TPC modes in graphene bilayers with a generic (non-minimal) stacking. These are known as twisted graphene bilayers, and are characterised by a finite interlayer rotation angle. We find that TPC modes may arise in these systems *without* strain under a *uniform* interlayer bias

$U$ . These chiral modes arrange into a triangular network of valley-polarized current running along zero mass lines [13]. This is a variation of what is commonly known as a Chalker-Coddington network [14–16]. Superimposed onto this delocalized network, a discrete set of states strongly localized away from AB'/BA' regions emerge at resonant energies. Such restructuring of electronic states occurs for energies  $|\epsilon| < |U|/2$ , and produces clearly measurable signatures in the density of states (DOS) and the optical conductivity  $\sigma_{xx}(\omega)$ . Interestingly, the mechanism that gives rise to the chiral network also appears, although for different reasons, in graphene monolayers on boron-nitride (h-BN) substrates [13, 17–19]. The lattice mismatch between graphene and h-BN, however, does not allow for an arbitrarily large Moiré period, so that unlike in twisted bilayers, the chiral network is not expected to fully develop in that case.

*Band topology and chiral modes.*—Let us briefly review some concepts on the band topology of graphene bilayers. Any electronic band defined in a finite Brillouin zone (BZ) has an associated integer topological invariant [11, 20–22], known as Chern number  $C$ , which determines e.g. its contribution to the Hall conductivity  $\sigma_{xy} = Ce^2/h$  when the band is completely filled [23–27]. In 2+1 dimensions, the Chern number is defined in terms of eigenstates  $|\psi(\mathbf{k})\rangle$  as  $C = \frac{1}{2\pi} \int_{BZ} d^2k F(\mathbf{k})$ , where  $F(\mathbf{k}) = 2\text{Im}\langle \partial_{k_x} \psi(\mathbf{k}) | \partial_{k_y} \psi(\mathbf{k}) \rangle$  is the Berry curvature. A biased AB'-stacked graphene bilayer develops a gap around its two valleys, located at points  $K$  and  $K'$  in the BZ. The Berry curvature of the valence band is peaked around these two points and has opposite sign, so that  $C = 0$ . However, a (non-quantized) valley Chern number may be defined by confining the  $\mathbf{k}$  integral to the region around a single valley,  $C_{K(\prime)} = \frac{1}{2\pi} \int_{K(\prime)} d^2k F(\mathbf{k})$ . If the bias is small as compared to the interlayer coupling,  $U < \gamma_\perp$ ,  $C_K = -C_{K'} \approx \text{sign}(U)$  is approximately quantised. This valley Chern number plays then the role of a proper topological charge [28], as long as valleys are kept decoupled by any perturbation (i.e. as long as the

bilayer, and  $U(\mathbf{r})$  itself, are smooth on the scale of the lattice constant  $a_0$ ). In particular, it implies the emergence of two TPC modes per valley and spin along an interface where  $U$  (and hence  $C_{K(\prime)}$ ) smoothly changes sign [8]. Likewise, since a BA'-stacking has opposite valley Chern numbers than AB' ( $C_{K(\prime)}^{AB'} = -C_{K(\prime)}^{BA'}$ ), a smooth transition between these two stackings will also produce two TPC modes per valley and spin [12]. This result is a version of the bulk-boundary correspondence, which states that  $N = |C_2 - C_1| \bmod 2$  TPC modes emerge where the Chern number changes from  $C_1$  to  $C_2$ . The mod 2 is absent in our case ( $N = 2$ ) since we consider only valley-preserving perturbations, hence "weak" topological protection, see Ref. 11. A transition between stackings arises naturally in a bilayer with a relative rotation between layers, the so-called twisted graphene bilayer.

*Continuum theory of twisted bilayers.*—A twisted graphene bilayer is parameterised by the relative rotation angle  $\theta$ , with  $\theta = 0$  denoting the AA' bilayer. Geometrically, such rotation produces a periodic triangular Moiré pattern in the local stacking, which smoothly alternates between the three minimal types AA', AB' and BA'. For an angle of rotation  $\theta < 30^\circ$ , the Moiré pattern has a period  $L_M = a_0 / [2 \sin(\theta/2)]$  ( $a_0 = 2.46\text{\AA}$  is the monolayer Bravais period). Electronically, the low energy sector of the system does not depend on the detailed crystallography [29–33], and is well described by a continuum theory in which the two valleys are decoupled, and the Dirac points in each layer are offset by a momentum  $\Delta K = 2|K| \sin(\theta/2)$ , with  $|K| = 4\pi/3a_0$ . In the absence of interlayer coupling, the two cones intersect around the M point of the superlattice, at energy  $\epsilon_M(\theta) = \hbar v_F \Delta K / 2$  (which is  $\approx 88\text{meV} \times \theta(\text{deg})$  for small angles). This is the natural energy scale in the low energy sector. The coupled bilayer is described within each valley by the continuum spin-degenerate Hamiltonian

$$H = \begin{pmatrix} U/2 & \hbar v_F \Pi_+^\dagger & V^*(\mathbf{r}) & V^*(\mathbf{r} - \delta\mathbf{r}) \\ \hbar v_F \Pi_+ & U/2 & V^*(\mathbf{r} + \delta\mathbf{r}) & V^*(\mathbf{r}) \\ V(\mathbf{r}) & V(\mathbf{r} + \delta\mathbf{r}) & -U/2 & \hbar v_F \Pi_-^\dagger \\ V(\mathbf{r} - \delta\mathbf{r}) & V(\mathbf{r}) & \hbar v_F \Pi_- & -U/2 \end{pmatrix}$$

which is written in the  $A, B, A', B'$  basis. Here  $\Pi_\pm = k_x + i(k_y \mp \Delta K/2)$ , and the function  $V(\mathbf{r}) = \frac{1}{3}\gamma_\perp \sum_{i=1}^3 e^{i\mathbf{g}_i \cdot \mathbf{r}}$  describes the periodic spatial variation of the interlayer coupling, with  $\gamma_\perp \approx 0.33\text{eV}$ . The Moiré lattice vectors are denoted by  $\mathbf{a}_{1,2}$  (so  $L_M = |\mathbf{a}_{1,2}|$ ), and conjugate momenta are  $\mathbf{g}_{1,2}$ , such that  $\mathbf{g}_i \cdot \mathbf{a}_j = 2\pi\delta_{ij}$  (we also define  $\mathbf{g}_3 = 0$ ). The AA' sublattice is centered at the origin, with the AB'/BA' sublattices offset by  $\pm\delta\mathbf{r} = (\mathbf{a}_1 - \mathbf{a}_2)/3$ .

The continuum model has two distinct regimes, depending on the value of dimensionless parameter  $\alpha(\theta) = \frac{1}{6}\gamma_\perp/\epsilon_M(\theta)$ . The regime of large angles ( $\theta \gg 1^\circ$ ,  $\alpha \ll 1$ ) is amenable to perturbation theory in  $\alpha$ , and has been extensively studied. It is characterised by the formation of a van-Hove singularity [29, 34–37] at energy

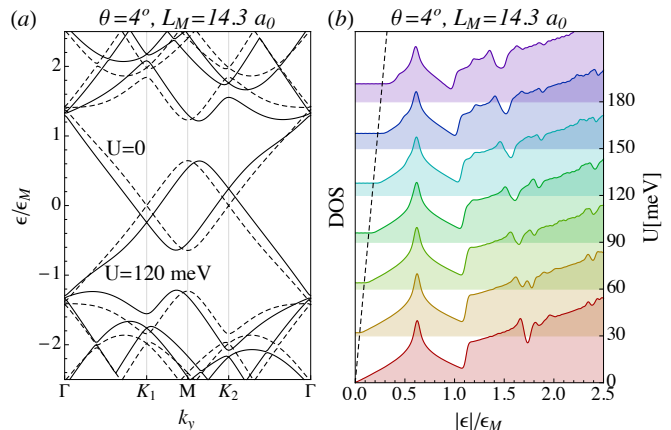


FIG. 1. (Color online) (a) Bandstructure and (b) density of states (DOS) for a  $\theta = 4^\circ$  twisted bilayer with and without interlayer bias  $U$ . At such angles, a bias merely shifts the two Dirac cones, creating a flat DOS plateau for  $|\epsilon| < |U|/2$  [to the left of the dashed line in (b)].

$\epsilon_{\text{vH}} \approx \epsilon_M(1 - 2\alpha)$  close to the M point [see peak in the DOS at  $\sim 0.6\epsilon_M$  in Fig. 1(b)] and a suppression of the Fermi velocity  $v_F^* \approx v_F(1 - 9\alpha^2)$  [29, 35]. In the presence of a finite bias  $U$ , the band structure in the large angle regime reacts in a predictable fashion, merely shifting the two Dirac cones by  $\pm U/2$ , see Fig. 1(a), since their eigenstates mostly reside in different layers in this case. This results in a low energy density of states that is flat instead of linear for  $|\epsilon| < |U|/2$ , see Fig. 1(b). The DOS profile is reminiscent of the perfect AA'-stacked bilayer's, whose band structure is also composed of two shifted Dirac cones. Above  $|U|/2$ , the DOS is largely unaffected by the bias.

The regime of small angles has been less explored and has a much more complex structure. In the unbiased case, secondary van Hove singularities above the first appear and move lower in energy as  $\theta$  is decreased. As each singularity approaches zero energy, it morphs into a quasi-flat miniband, which is accompanied by a vanishing Fermi velocity  $v_F^*$ . This occurs at specific ("magic") twist angles  $\theta_i$ , the highest being  $\theta_1 \approx 1.05^\circ$  (which corresponds to  $L_M \approx 52a_0$ ) [38, 39]. In general however, this simple picture can only make sense of the spectrum for angles down to around  $\theta \sim 0.35^\circ$ . Below this  $\theta$ , the  $U = 0$  electronic structure becomes rather intricate. With the notable exception of a resilient AA'-localized state [40, 41] pinned at around  $\epsilon \sim 0.17\epsilon_M$  (which is evolved from the original large angle van-Hove singularity), the DOS profile, as shown in the bottom curve of Fig. 2(a), exhibits no clear structure (although see Ref. 39), and states are typically delocalised (Fig. 2(f)).

The small-angle electronic structure becomes much simpler as  $U$  is increased. The AB' and BA' regions develop a local gap, with opposite valley Chern number. If  $U$  is above certain threshold, and these regions are large

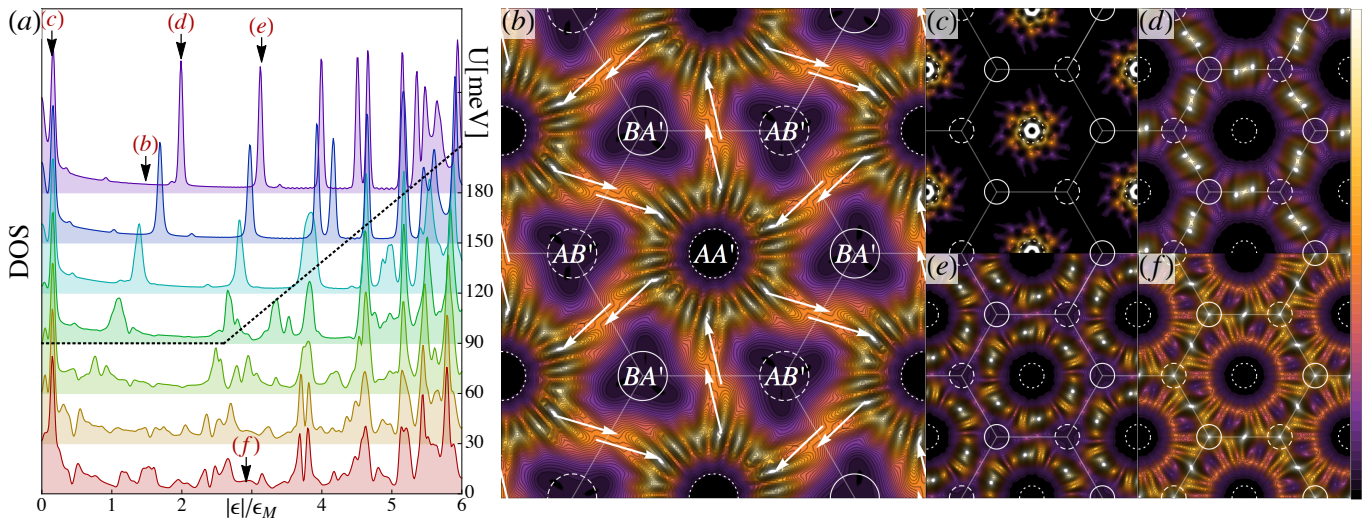


FIG. 2. (Color online) (a) Density of states of a  $L_M = 290a_0$  ( $\theta \approx 0.2^\circ$ ) twisted bilayer with increasing bias  $U$ . The region above the dotted line denotes the chiral network regime. (b-f) Periodic spatial profile of electron probability density for several characteristic eigenstates in the spectrum [arrows in (a)], all chosen at one of the  $K$  points. Black colour corresponds to zero density, and white to maximum. Panel (b) shows a fully developed chiral network (Chalker-Coddington) state, with arrows indicating the orientation of the valley currents. Panels (c), (d) and (e) show various resonant states, all localized away from  $AB'/BA'$  regions by the finite bias. Panel (f) shows a  $U = 0$  delocalized state.

enough (small enough angles), the bias tends to electronically deplete them. As a consequence, strong confinement of states away from the depleted  $AB'/BA'$  regions becomes possible. A discrete set of sharp localized resonances appear in the spectrum, as seen in the top curve of Fig. 2(a). These localized states arrange spatially in a variety of patterns [see Fig. 2(c,d,e)], but always away from the  $AB'/BA'$  regions. For off-resonant energies, the DOS exhibits a weak and featureless background that is in marked contrast to the intricate small-angle,  $U = 0$  DOS profile, and to the Dirac-like linear background of the large-angle DOS. This weak background corresponds to delocalized TPC modes running along  $AB'/BA'$  interfaces, which develop due to the spatial modulation in the valley Chern number of the gapped regions. The collection of chiral channels arrange in a triangular Chalker-Coddington chiral network, as shown in Fig. 2(b). Each channel carries opposite current for opposite valleys. The pattern of valley currents for a given sign of  $U$  is fixed by the band topology, and is shown by white arrows.

This new electronic phase requires strong depletion in  $AB'$  and  $BA'$  regions to fully develop [13], which in turn requires large bias and small angles. One can approximately quantify this condition by considering the simplified one-dimensional problem of an abrupt  $AB'/BA'$  interface with a uniform bias. Using the two component approximation (valid for  $U < \gamma_\perp$ ), an interface mode decays like  $\sim e^{-\lambda|x|}$ , with  $\lambda = \sqrt{U\gamma_\perp}/2v_F$  [8]. We look for the value of  $U$  that results in an amplitude decay of the interface mode of at least, say, 95%, within the radius of the Moiré  $BA'$  region of the twisted bilayer,

$R = L_M/2\sqrt{3}$ . This is half the distance between  $AB'$  and  $BA'$  region centers, see Fig. 2(b). Inserting  $x = R$  this results in the following condition for the development of the chiral network

$$p^2 \left( \frac{l_\perp}{L_M(\theta)} \right)^2 < \frac{U}{\gamma_\perp} < 1, \quad |\epsilon| < \frac{|U|}{2} \quad (1)$$

where  $p = -4\sqrt{3} \log 0.05 = 20.76$ , and  $l_\perp = \hbar v_F/\gamma_\perp \approx 7.3a_0$  is the interlayer coupling length [42].

This analysis suggests that for a realistic value of  $U \sim 90$  meV, the network requires a Moiré period  $L_M \gtrsim 290a_0$  ( $\theta < 0.2^\circ$ ), the value chosen in Fig. 2. For this angle, the range of  $U$  and  $\epsilon$  that satisfies the criterion has been marked by a dotted boundary in Fig. 2(a). We see the boundary roughly correlates with the crossover into the chiral network regime, characterised by sharp DOS peaks on a weak smooth background.

The DOS depends only on the density of energy eigenvalues of the system. Other equilibrium observables, such as the optical conductivity  $\sigma_{xx}(\omega)$ , contain additional information related to matrix elements between different eigenstates. It can be computed using the Kubo formula

$$\sigma_{xx}(\omega) = \frac{ie^2}{\omega} \int d\epsilon d\epsilon' \frac{n_F(\epsilon) - n_F(\epsilon')}{\hbar\omega - \epsilon' + \epsilon + i0} F(\epsilon, \epsilon'), \quad (2)$$

where  $F(\epsilon, \epsilon') = \text{Tr} [\delta(\epsilon - H) j_x \delta(\epsilon' - H) j_x]$ , and  $j_x$  is the current operator in the  $x$  direction. Quite famously, the low-frequency limit of the optical conductivity is universal in a neutral graphene monolayer  $\sigma_{xx}(\omega \rightarrow 0) = \sigma_0 \equiv \frac{\pi}{2} \frac{e^2}{h}$ , which corresponds to a universal infrared transmission at normal incidence  $T = (1 + \pi\alpha/2)^{-2} \approx 97.7\%$ , in

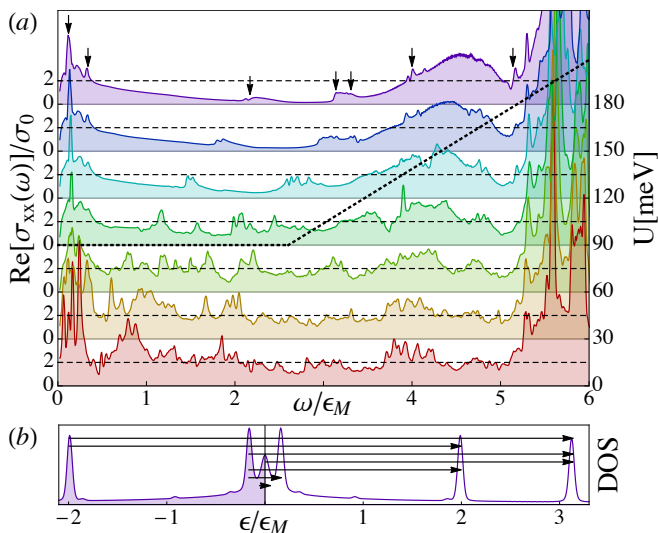


FIG. 3. (Color online) (a) Zero-temperature optical conductivity  $\text{Re}[\sigma(\omega)]$  at neutrality ( $\mu = 0$ ) for increasing bias  $U$  and twist angle like in Fig. 2. It exhibits complex fluctuations around  $2\sigma_0 = \pi e^2/h$  at small  $U$  (dashed line). As the system transitions into the chiral network phase (above thick dotted line), the fluctuations are transformed into a smooth, non-monotonous background corresponding to transitions between chiral states, with weak superimposed resonances from transitions between localised states. Some of the latter [arrows in (a)] are shown in (b) for  $U = 180$  meV and increasing frequency [arrows from bottom to top].

terms of the fine structure constant  $\alpha$  [43, 44]. In an unbiased, large-angle twisted bilayer,  $\sigma_{xx}(\omega)$  exhibits features associated to the van-Hove singularities [45–47]. As the system enters the low-angle regime, the optical conductivity exhibits a complexity similar to the DOS, in the form of fluctuations around a rough average of  $2\sigma_0$  (which corresponds to two decoupled monolayers). Under an increasing interlayer bias, however,  $\sigma_{xx}(\omega)$  becomes remarkably simple, like the DOS, see Fig. 3. It evolves into a smooth background that is non-monotonous in  $\omega$ , and which falls below  $2\sigma_0$ , representing the optical absorption of the delocalised chiral network. This background exhibits superimposed peaks that reflect transitions between sharp localised states [see arrows in panels (a) and (b)]. Such peaks, however, are much suppressed as compared to those in the DOS, due to the small overlap of localised eigenfunctions under the action of the current operator  $j_x$ . Hence, absorption due to the chiral network becomes the dominant feature of  $\sigma_{xx}(\omega)$  at low frequencies. For frequencies larger than  $|U|/2$ , complex features are still present, of a magnitude similar to those of the unbiased case.

In conclusion, we have shown that an interlayer bias generates a starkly different low energy electronic structure for Bernal-stacked, AA'-stacked and twisted bilayer graphene. While the former are semiconducting and metallic, respectively, the latter develops a novel spectral

structure at low twist angles and realistic values of the bias, as a consequence of the depletion of AB' and BA'-type regions in the Moiré pattern. The periodic modulation of the local band topology gives rise to the formation of a delocalized chiral network of protected states of the Chalker-Coddington type, whose density of states is smooth and decreasing up to energy  $\pm|U|/2$ . Localized states also appear at specific resonant energies in various spatial configurations away from the depleted AB'/BA' regions. These features are visible both in the spectral density and in the optical conductivity, which become strongly modified as the bias exceeds the threshold for the formation of the chiral network phase.

We acknowledge financial support from the Spanish Ministry of Economy (MINECO) through the Ramón y Cajal programme, Grant no. FIS2010-21883 (E. P.), and Grant no. FIS2011-23713, and from the European Research Council Advanced Grant, contract 290846 (P. S.-J.).

- 
- [1] A. H. C. Neto, F. Guinea, N. M. R. Peres, K. S. Novoselov, and A. K. Geim, *Rev. Mod. Phys.* **81**, 109 (2009).
  - [2] The notation for minimal graphene stackings refers to the four carbon atoms A, B, A' and B' of the minimal unit cell of the bilayer. Thus, AB' stacking refers to the case in which the A carbon in the lower layer is vertically aligned with the B atom in the upper layer, whilst AA' has both A and B atoms of each layer vertically aligned. Clearly, non-minimal stackings are also possible, such as that of a generic twisted bilayer.
  - [3] E. McCann, *Phys. Rev. B* **74**, 161403 (2006).
  - [4] E. V. Castro, K. S. Novoselov, S. V. Morozov, N. M. R. Peres, J. M. B. L. dos Santos, J. Nilsson, F. Guinea, A. K. Geim, and A. H. C. Neto, *J. Phys.: Condens. Matter* **22**, 175503 (2010).
  - [5] K. F. Mak, C. H. Lui, J. Shan, and T. F. Heinz, *Phys. Rev. Lett.* **102**, 256405 (2009).
  - [6] Y. Zhang, T.-T. Tang, C. Girit, Z. Hao, M. C. Martin, A. Zettl, M. F. Crommie, Y. R. Shen, and F. Wang, *Nature* **459**, 820 (2009).
  - [7] E. V. Castro, K. S. Novoselov, S. V. Morozov, N. M. R. Peres, J. M. B. L. dos Santos, J. Nilsson, F. Guinea, A. K. Geim, and A. H. C. Neto, *Phys. Rev. Lett.* **99**, 216802 (2007).
  - [8] I. Martin, Y. Blanter, and A. Morpurgo, *Phys. Rev. Lett.* **100**, 36804 (2008).
  - [9] The chiral property of protected modes in the context of graphene bilayers is the fixed relation between their direction of propagation along the boundary and their valley quantum number.
  - [10] X.-L. Qi, T. L. Hughes, and S.-C. Zhang, *Phys. Rev. B* **78**, 195424 (2008).
  - [11] M. Z. Hasan and C. L. Kane, *Rev. Mod. Phys.* **82**, 3045 (2010).
  - [12] A. R. Wright and T. Hyart, *Appl. Phys. Lett.* **98**, 251902 (2011).
  - [13] T. Tudorovskiy and M. I. Katsnelson, arXiv:1206.2244.

- [14] J. T. Chalker and P. D. Coddington, *J. Phys. C: Solid State Phys.* **21**, 2665 (1988).
- [15] C.-M. Ho and J. T. Chalker, *Phys. Rev. B* **54**, 8708 (1996).
- [16] V. V. Mkhitarian and M. E. Raikh, *Phys. Rev. B* **79**, 125401 (2009).
- [17] B. Sachs, T. O. Wehling, M. I. Katsnelson, and A. I. Lichtenstein, *Phys. Rev. B* **84**, 195414 (2011).
- [18] L. A. Ponomarenko, R. V. Gorbachev, D. C. Elias, G. L. Yu, A. S. Mayorov, J. Wallbank, M. Mucha-Kruczynski, A. Patel, B. A. Piot, M. Potemski, I. V. Grigorieva, K. S. Novoselov, F. Guinea, V. I. Fal'ko, and A. K. Geim, (2012), 1212.5012.
- [19] M. Mucha-Kruczynski, J. Wallbank, and V. Fal'ko, arXiv:1304.1734.
- [20] J. E. Avron, R. Seiler, and B. Simon, *Phys. Rev. Lett.* **51**, 51 (1983).
- [21] J. Zak, *Phys. Rev. Lett.* **62**, 2747 (1989).
- [22] D. Xiao, M.-C. Chang, and Q. Niu, *Rev. Mod. Phys.* **82**, 1959 (2010).
- [23] R. B. Laughlin, *Phys. Rev. B* **23**, 5632 (1981).
- [24] D. J. Thouless, M. Kohmoto, M. P. Nightingale, and M. den Nijs, *Phys. Rev. Lett.* **49**, 405 (1982).
- [25] M. Kohmoto, *Annals of Physics* **160**, 343 (1985).
- [26] M. Kohmoto, *Phys. Rev. B* **39**, 11943 (1989).
- [27] J. E. Avron, D. Osadchy, and R. Seiler, *Physics today* **56**, 38 (2003).
- [28] E. Prada, P. San-Jose, L. Brey, and H. Fertig, *Solid State Commun.* **151**, 1075 (2011).
- [29] J. M. B. L. dos Santos, N. M. R. Peres, and A. H. Castro Neto, *Phys. Rev. Lett.* **99**, 256802 (2007).
- [30] E. J. Mele, *Phys. Rev. B* **81**, 161405 (2010).
- [31] E. J. Mele, *Phys. Rev. B* **84**, 235439 (2011).
- [32] R. de Gail, M. O. Goerbig, F. Guinea, G. Montambaux, and A. H. Castro Neto, *Phys. Rev. B* **84**, 045436 (2011).
- [33] J. M. B. L. dos Santos, N. M. R. Peres, and A. H. C. Neto, *Phys. Rev. B* **86**, 155449 (2012).
- [34] G. Li, A. Luican, J. M. B. Lopes dos Santos, A. H. Castro Neto, A. Reina, J. Kong, and E. Y. Andrei, *Nat Phys* **6**, 109 (2010).
- [35] A. Luican, G. Li, A. Reina, J. Kong, R. R. Nair, K. S. Novoselov, A. K. Geim, and E. Y. Andrei, *Phys. Rev. Lett.* **106**, 126802 (2011).
- [36] W. Yan, M. Liu, R.-F. Dou, L. Meng, L. Feng, Z.-D. Chu, Y. Zhang, Z. Liu, J.-C. Nie, and L. He, *Phys. Rev. Lett.* **109**, 126801 (2012).
- [37] I. Brihuega, P. Mallet, H. González-Herrero, G. T. de Laissardière, M. M. Ugeda, L. Magaud, J. M. Gómez-Rodríguez, F. Ynduráin, and J.-Y. Veuillen, (2012), arXiv:1209.0991v1.
- [38] R. Bistritzer and A. H. MacDonald, *PNAS* **108**, 12233 (2011).
- [39] G. T. de Laissardière, D. Mayou, and L. Magaud, *Phys. Rev. B* **86**, 125413 (2012).
- [40] G. T. de Laissardière, D. Mayou, and L. Magaud, *Nano Lett.* **10**, 804 (2010).
- [41] P. San-Jose, J. González, and F. Guinea, *Phys. Rev. Lett.* **108**, 216802 (2012).
- [42] I. Snyman and C. W. J. Beenakker, *Phys. Rev. B* **75**, 045322 (2007).
- [43] T. Stauber, N. M. R. Peres, and A. K. Geim, *Phys. Rev. B* **78**, 085432 (2008).
- [44] R. R. Nair, P. Blake, A. N. Grigorenko, K. S. Novoselov, T. J. Booth, T. Stauber, N. M. R. Peres, and A. K. Geim, *Science* **320**, 1308 (2008).
- [45] P. Moon and M. Koshino, arXiv:1302.5218.
- [46] C. J. Tabert and E. J. Nicol, arXiv:1302.7233.
- [47] X. Zou, J. Shang, J. Leaw, Z. Luo, L. Luo, C. La-o vorakiat, L. Cheng, S. A. Cheong, H. Su, J.-X. Zhu, Y. Liu, K. P. Loh, A. H. Castro Neto, T. Yu, and E. E. M. Chia, *Phys. Rev. Lett.* **110**, 067401 (2013).